The effect of heat treatments on the structure and magnetic properties of melt-spun $Co_{10}Cu_{90}$ ribbons

2002 J. Phys.: Condens. Matter 14 7513

(http://iopscience.iop.org/0953-8984/14/32/311)

INSTITUTE OF PHYSICS PUBLISHING JOURNAL OF PHYSICS: CONDENSED MATTER

J. Phys.: Condens. Matter **14** (2002) 7513–7523 PII: S0953-8984(02)37532-5

The effect of heat treatments on the structure and magnetic properties of melt-spun $Co_{10}Cu_{90}$ ribbons

J Vergara and V Madurga

Departamento de Física, Universidad Pública de Navarra, Campus de Arrosadía s/n, E-31006, Pamplona, Spain

E-mail: jvergara@unavarra.es

Received 29 May 2002
Published 2 August 2002
Online at stacks.iop.org/JPhysCM/14/7513

Abstract

The changes in the nanostructure and magnetic and magnetotransport properties of $Co_{10}Cu_{90}$ melt-spun ribbons upon heating them have been measured. Thermal treatments to 650 K do not produce changes either in the x-ray diffraction patterns or in the magnetization isotherms of the ribbons. However, upon heating the samples above 650 K, a contraction of the Cu lattice, an irreversible decrease of their resistivity and an increase of the giant magnetoresistance (GMR) of the heated samples are observed. The largest value of the GMR (7% at 77 K and in a magnetic field of 8×10^5 A m^{-1}) is reached in samples heated to 850 K. These results are explained by assuming the nucleation and growth of superparamagnetic Co nanoclusters in the Cu-rich matrix. The magnetic moment of these clusters was estimated to be 10^4 μ_B. Thermal treatments above 850 K produce an increase of the magnetic moment of the samples (in magnetic fields of 8×10^5 A m^{-1}) and of their coercivity, although the value of the GMR decreases. Parallel to these changes, the intensity of the x-ray diffraction peaks for Co increases. Further growth of the Co nanoclusters is responsible for the changes of the magnetic moment and GMR of the samples.

(Some figures in this article are in colour only in the electronic version)

1. Introduction

The study of granular alloys composed of magnetic clusters either in a conductive or in an insulating matrix has recently attracted a great deal of attention since the observation of novel properties such as giant magnetoresistance (GMR) [1, 2], tunnel magnetoresistance [3] and the giant Hall effect [4].

Magnetic granular materials consist of a dispersion of magnetic particles, whose sizes are in the region of a few nanometres, which are embedded in a conductive matrix. As a

consequence of this particular nanostructure, the high surface-to-volume ratio of the magnetic particles becomes an important factor that lies at the origin of the special properties exhibited by these systems [5, 6].

These nanocrystalline compounds may be obtained by different methods, such as sputtering [7], melt-spinning [8, 9], electrodeposition [10], mechanical alloying [11] and pulsed laser ablation deposition [12]. In the particular case of the Co–Cu system, Co has been reported to be practically insoluble in Cu: only 0.3% Co may be dissolved in a Cu matrix at 500 °C [13]. Thus, it is necessary to make use of one of the former techniques, which involve fast quenching rates, to increase the concentration of Co in the Cu matrix. As a result of these fast quenching rates, metastable compounds are originated [14]: the concentration of Co in these CoCu compounds lies above the concentration for thermodynamic equilibrium at room temperature. A subsequent heat treatment was reported to give rise to the growth of small Co clusters in the Cu matrix [15]. In particular, for the Co–Cu system, the highest values of the GMR have been reported when the samples were subjected to annealing processes [16].

In this work we have measured the changes of both the structure and magnetic properties of melt-spun $Co_{10}Cu_{90}$ ribbons upon heating the samples. A correlation between the changes in the x-ray diffraction patterns, transport and magnetic properties is presented, as well as a possible explanation of these changes, based on the modifications of the nanostructure of the melt-spun ribbons. Although similar results and conclusions have already been reported in the literature [17, 18], this work provides new experimental evidence (x-ray diffraction and magnetothermogravimetric measurements) to support the hypothesis that the nucleation and growth of Co nanoparticles lies at the origin of the changes of the magnetic and transport properties of $Co_{10}Cu_{90}$ melt-spun ribbons.

2. Experimental details

Granular $Co_{10}Cu_{90}$ ribbons were fabricated by rapid solidification in a home-made melt-spinner in a controlled Ar (99.999%) atmosphere. The $Co_{10}Cu_{90}$ ingot used to produce the melt-spun ribbons was obtained by melting pure Co (99.8%) and pure Cu (99.75%) powders in an induction furnace [19]. Heat treatments to 1250 K, of the as-quenched samples, were carried out either in a magnetothermogravimetric analyser (TGA-7 Perkin-Elmer) or inside a common furnace. In both cases, a continuous flux of Ar gas was used to avoid oxidation of the samples. The heating rate was of the order of 20 K min^{-1}. The samples were kept for one minute at the given annealing temperature.

The structure of the samples was measured in an x-ray diffractometer (XRD-3000, Seifert) in the θ–2θ configuration. A Mo tube ($\lambda = 0.070\,93$ nm) and a secondary monochromator were used for these measurements.

The magnetic moment of the samples was measured with a vibrating sample magnetometer both at room temperature and in magnetic fields to 8×10^5 A m^{-1}. Also, in the temperature range from 300 to 1250 K, a magnetothermogravimetric analyser (TGA-7, Perkin-Elmer) measured the magnetic force exerted by a horseshoe magnet on the samples. The average magnetic field applied to the samples was 1.2×10^4 A m^{-1}.

The GMR of the samples was measured with the standard four-point probe technique in magnetic fields to 8×10^5 A m^{-1} from 4 K to room temperature, with an ac (75 Hz) resistance bridge (F26 model, ASL). The resistivity of the samples was measured on heating the $Co_{10}Cu_{90}$ ribbons to 900 K in a conventional furnace in an Ar atmosphere.

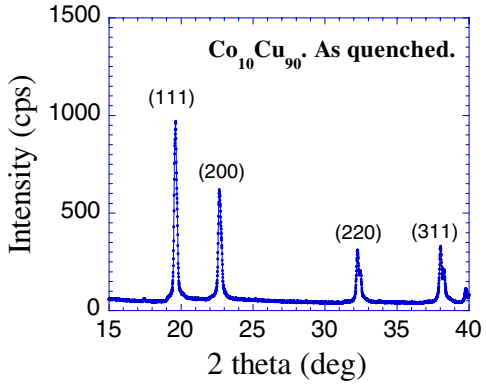

Figure 1. The x-ray diffraction pattern of the as-quenched $Co_{10}Cu_{90}$ ribbon. The plane indices indicated in the figure correspond to those of fcc Cu.

Table 1. Values of the 2θ angles of the x-ray diffraction maxima and lattice parameters for bulk fcc Cu and for as-quenched and heat-treated $Co_{10}Cu_{90}$ melt-spun ribbon.

Material	Position of the (111) diffraction peak (deg)	Lattice parameter (Å)
Pure bulk fcc Cu	19.57	3.615
As-quenched $Co_{10}Cu_{90}$	19.52	3.624
$Co_{10}Cu_{90}$ heated to 660 K	19.54	3.620
$Co_{10}Cu_{90}$ heated to 700 K	19.55	3.618
$Co_{10}Cu_{90}$ heated to 800 K	19.56	3.6165

3. Results and discussion

The changes in the nanostructure and transport and magnetic properties of $Co_{10}Cu_{90}$ melt-spun ribbons upon heat treatment are explained throughout this section.

As detailed above, Co is practically immiscible in Cu at room temperature. Only by ultrafast quenching can a certain amount of Co be dissolved in the Cu matrix, leading to the formation of a metastable compound [13]. The x-ray diffraction pattern corresponding to the as-quenched sample is displayed in figure 1. As a consequence of the low concentration of Co in the samples, only the diffraction maxima close to the maxima of bulk fcc Cu are observed. However, the positions of the diffraction peaks for the as-quenched $Co_{10}Cu_{90}$ sample do not exactly agree with those for bulk Cu: the diffraction peaks for the as-quenched $Co_{10}Cu_{90}$ ribbon are slightly displaced towards lower 2θ angles, which indicates that on average, the Cu-rich matrix is expanded, probably due to the presence of Co atoms or defects, within the Cu-rich crystallites (see table 1).

No significant changes in the nanostructure or in the magnetic and transport properties take place on heating the melt-spun $Co_{10}Cu_{90}$ ribbons to temperatures of the order of 650 K.

However, heat treatments above the former temperature induce changes in the structure and in the transport and magnetic properties of the ribbons. For instance, on increasing the heating temperature, the position of the x-ray diffraction peaks from the samples heated in the temperature range from 650 to 800 K approach the positions for pure bulk fcc Cu; cf figure 2(a) and table 1. According to Bragg's law, the former result indicates that on heating the samples, the lattice parameter of the Cu-rich matrix decreases and becomes closer to that

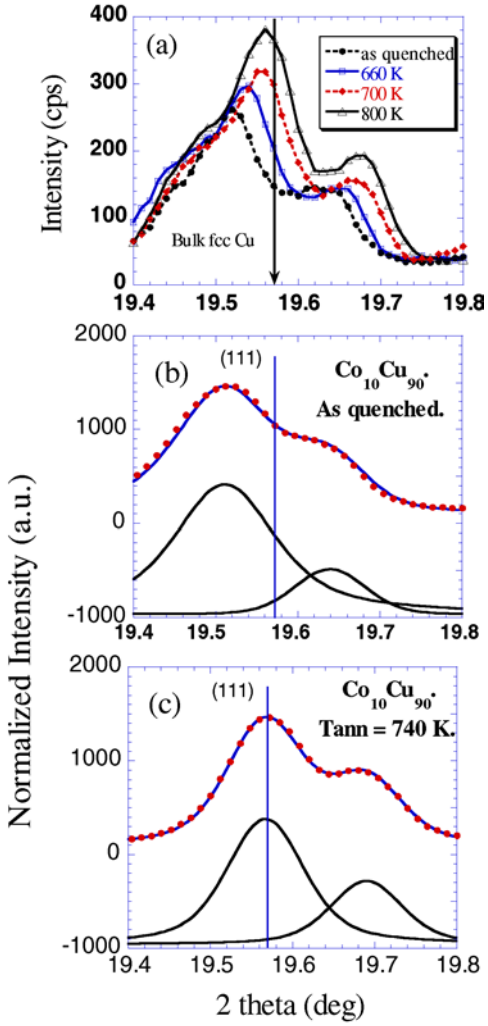

Figure 2. Details of the diffraction maximum corresponding to (111) planes for the as-deposited and heat-treated $Co_{10}Cu_{90}$ samples (a). Dashed and solid curves in (a) are a guide to the eyes. Fits of the normalized x-ray diffraction pattern for the $Co_{10}Cu_{90}$ as-quenched sample (b) and the sample heated to 740 K (c) to pseudo-Voigt functions (solid curves for the fits and dots for the experimental data points). The straight line, in all plots, indicates the position of the diffraction maximum of the (111) planes of bulk fcc Cu.

of pure Cu. This indicates that the Cu-rich matrix becomes progressively free from impurities and defects, as a consequence of the heat treatments. Parallel to the former contraction, an increase of the intensity of the diffraction maxima as well as a narrowing of the diffraction peaks are observed in the x-ray patterns of the heated samples—cf figure 2(a)—which is the fingerprint of an increase of the grain size of the Cu crystals. In order to determine the size of the former grains, we have fitted the diffraction maxima of the fcc Cu(111) planes of both the as-quenched (figure 2(b)) and the 740 K annealed sample (figure 2(c)) to pseudo-Voigt functions [20]. Both, the $K\alpha_1$ and $K\alpha_2$ lines from Mo were taken into account. From this fit

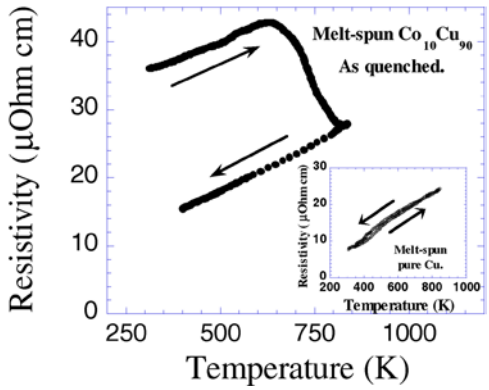

Figure 3. The temperature dependence of the resistance of the as-quenched $Co_{10}Cu_{90}$ sample. The inset represents the thermal evolution of the resistance of a pure Cu melt-spun ribbon.

and according to the Scherrer formula [21]:

$$t = \frac{0.9\lambda}{B\cos\theta_B} \tag{1}$$

where B is the full width at half-maximum (FWHM), θ_B is half the angle of the diffraction maximum and λ the wavelength of the radiation, the size of the Cu crystals increases from 23 nm in the as-quenched sample to 34 nm in the 740 K annealed one.

Parallel to the former structural changes, an irreversible decrease of the resistance is observed in the temperature range from 650 to 820 K (figure 3). Above 820 K, no further irreversible changes in the resistance are observed on warming the ribbons to 950 K. Although this irreversible decrease in resistance would mainly take place in the Cu matrix, the presence of Co in the samples is the key factor for this behaviour. Previously, the resistivity of a pure Cu melt-spun ribbon was measured as the sample was heated to 900 K, as displayed in the inset of figure 3. No irreversible change of the resistivity took place on heating the pure Cu ribbon to 900 K.

A close connection between the changes in the structure and resistivity of the $Co_{10}Cu_{90}$ melt-spun ribbons seems to be present, according to the previous results. On heating the samples, larger Cu crystallites are formed, which, in addition, show a lattice parameter closer to that of pure bulk Cu. The electron mean free path is thus increased in the Cu matrix, as it becomes free from defects and impurities (presumably Co atoms). Consequently the resistivity decreases. Thus, these changes are due to the presence of Co in the samples.

On heating the samples in the temperature range from 650 to 850 K, the GMR of the melt-spun $Co_{10}Cu_{90}$ ribbons also increases, as shown in figure 4. The maximum value of the GMR is reached after a heat treatment to 850 K (GMR measured at 77 K and in magnetic fields of the order of 8×10^5 A m^{-1}). The formation of small Co clusters from Co atoms that could be dispersed in the Cu-rich matrix, or the growth of smaller Co nanoaggregates, which takes place upon heating the samples at temperatures from 650 to 850 K, would give rise to the increase of the GMR.

The Co clusters responsible for the observation of the GMR behave like superparamagnetic particles [9, 16, 18]. The connection between superparamagnetism and GMR is evidenced by the low-temperature measurements of this transport property, as displayed in figure 5. The GMR of the $Co_{10}Cu_{90}$ ribbon annealed at 870 K shows a non-hysteretic behaviour to temperatures of the order of 20 K. Below this temperature, which can be considered as the

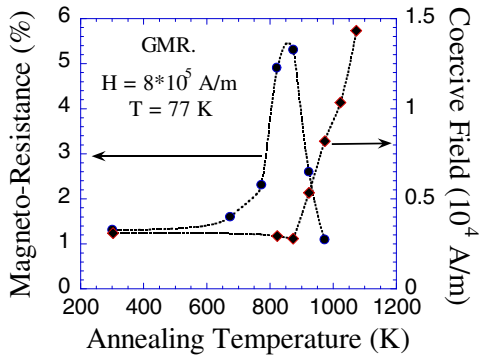

Figure 4. The dependence of the coercivity (measured at room temperature) and of the GMR of the $Co_{10}Cu_{90}$ ribbons on the heating temperature. Dashed curves are a guide to the eyes.

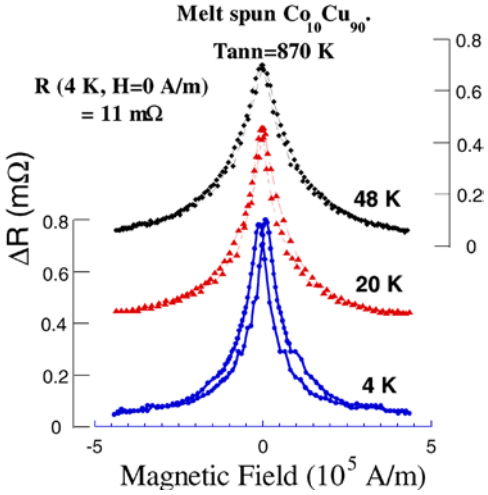

Figure 5. The magnetoresistance at low temperatures for the $Co_{10}Cu_{90}$ sample heated to 870 K. Curves are a guide to the eyes.

blocking temperature of the superparamagnetic particles, T_b, the GMR becomes hysteretic. According to [22] the blocking temperature is defined as

$$KV = 25k_BT_b \tag{2}$$

where K is the anisotropy constant, V is the volume of the magnetic particles, k_B is the Boltzmann constant and T_b represents the blocking temperature. A splitting of the GMR peaks is observed at low temperatures, which indicates that the magnetic particles that contribute to the GMR are blocked, as a consequence of the decrease of the thermal energy. The volume of these particles may be estimated by measuring the blocking temperature and the extrapolation to a null temperature of the coercive field. From the GMR measurements at low temperatures, the magnetic field necessary to achieve the maximum resistance, i.e. the highest degree of magnetic disorder, is considered to be the coercive field. For a system of blocked particles with uniaxial anisotropy, whose easy magnetization axes are randomly oriented, the coercivity is defined as [23–25]

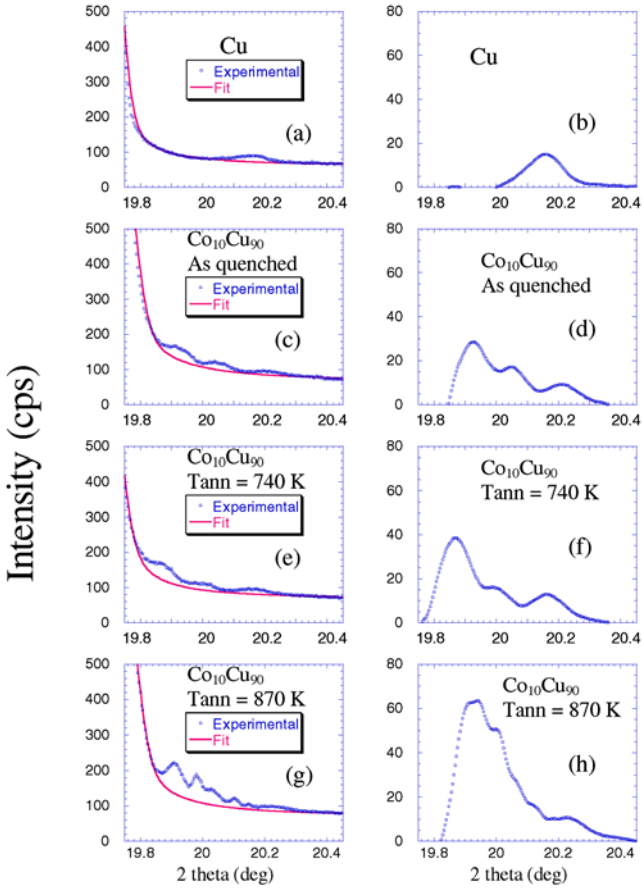

Figure 6. Details of the x-ray diffraction pattern for the pure Cu melt-spun ribbon ((a), (b)). The details of the contribution of Co in the x-ray diffraction pattern for the as-quenched $Co_{10}Cu_{90}$ sample are represented in (c) and (d); for the sample heated to 740 K in (e) and (f); and for the one heated to 870 K in (g) and (h). The solid curves represent the fit to a pseudo-Voigt functions. The contribution of Co is shown by the differences between the experimental data and the fits in (b), (d), (g) and (h).

$$H_c(T) = \frac{0.96K}{\mu_0 M_s}\left(1 - \frac{T}{T_b}\right)^{0.77}. \tag{3}$$

By making use of expressions (2) and (3) and assuming the extrapolated value of the coercivity to zero temperature to be 4×10^4 A m^{-1}, close to those for similar granular melt-spun ribbons with a Cu-rich matrix [25], the magnetic moment of the Co particles in the sample annealed to 870 K is of the order of 10^4 μ_B. And also, assuming that the magnetic moment of the Co atoms in these clusters is similar to that of Co atoms in the bulk, the size of these clusters would be roughly 5 nm.

Heat treatments at temperatures above 850 K give rise to significant changes mainly in the magnetic moment of the melt-spun ribbons, and in their nanostructure too.

These structural changes upon heat treatments are mainly manifested by an increase in the intensity of the diffraction peaks of the Co as displayed in figure 6. In this figure, both the details of the experimental data and the fit of the fcc Cu(111) peaks to pseudo-Voigt functions

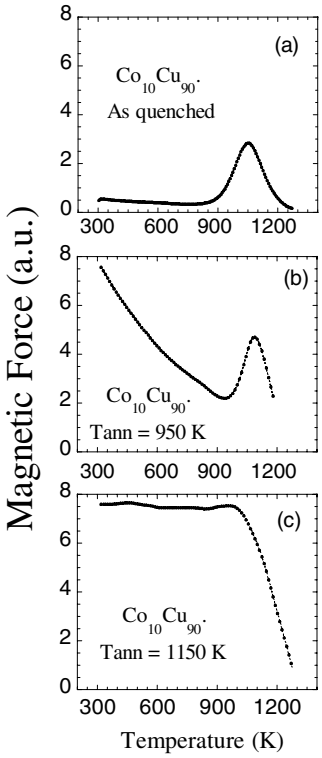

Figure 7. Magnetothermogravimetric patterns from the as-quenched $Co_{10}Cu_{90}$ melt-spun ribbon (a), and the ones heated to 950 K (b) and 1150 K (c). In all cases, the applied magnetic field is 1.2×10^4 A m^{-1}.

are displayed. The difference between these two curves corresponds to the contribution of Co—cf figures 6(d), (f) and (h). The x-ray diffraction pattern of pure Cu melt-spun ribbon in the as-quenched state is represented in figures 6(a) and (b).

The presence of Co is evidenced in figure 6 by the peaks that appear roughly at 2θ values of 19.9° and 20°, which correspond to the fcc Co(111) maxima produced by the Kα_1 and Kα_2 Mo lines. Also, a spurious peak appears at 20.2°, although this may not be attributed to Co as it also appears in the x-ray diffraction pattern of the pure Cu ribbon. A slight increase in the intensity of the Co peaks was observed when a heat treatment at 740 K was carried out. Nonetheless, the largest increase in the intensity of the Co peaks took place in the sample heated to 870 K, which would indicate a further growth of the size of the Co crystals.

Related to the changes in the magnetic moment of the ribbons, figure 7(a) displays the temperature dependence of the magnetic force experienced by the $Co_{10}Cu_{90}$ as-quenched sample in a magnetic field, which, on average, is of the order of 1.2×10^4 A m^{-1}. This magnetic force is directly related to the value of the magnetic moment of the sample in an applied magnetic field of 1.2×10^4 A m^{-1}. In the temperature range from 300 to 800 K, the former magnetic force decreases monotonically and in a reversible way. This behaviour could follow the thermal evolution of an ensemble of superparamagnetic particles. Above 800 K, an irreversible increase of the magnetic force of the sample takes place: the value of this magnetic force increases by almost one order of magnitude and reaches its maximum value at 1050 K. Above this temperature the magnetic force decreases again and vanishes at a temperature of about 1300 K, which is slightly below the Curie temperature of bulk Co (1398 K).

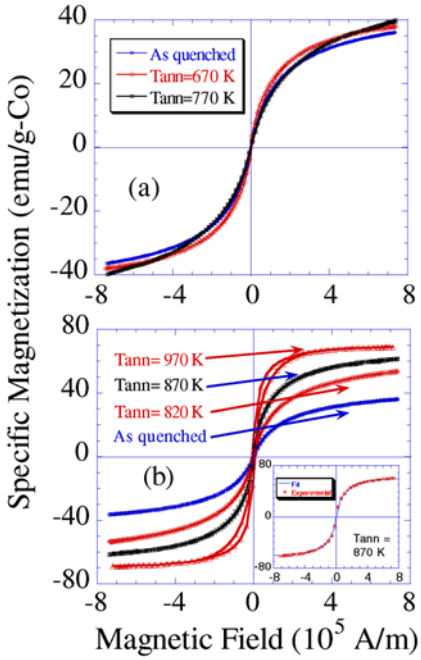

Figure 8. Magnetization isotherms (measured at 300 K) for the $Co_{10}Cu_{90}$ ribbons heated to temperatures below 800 K (a) and above 800 K (b). The inset of (b) represents both the experimental data and the fit (solid curve) to the Langevin function for the sample annealed at 870 K.

This result could be understood under the assumption of a further growth of Co nanocrystals within the Cu matrix. As the heating temperature is increased, so also is the atomic mobility, and consequently the Co atoms could group and form larger clusters. The magnetic moment of the samples would be enhanced due to the contribution of the Co atoms that would initially lie in the Cu matrix and, after a heat treatment, could displace to the vicinity of Co clusters that consequently would increase in size.

Magnetothermogravimetric measurements on the heated samples are also displayed in figures 7(b) and (c). The magnetic force experienced by the sample heated to 950 K also shows an irreversible increase roughly at this temperature. This magnetic force now reaches a relative maximum at 1050 K, similar to the one previously observed for the as-quenched sample. On heating the samples to 1150 K, all the structural transformations seem to have taken place, as shown in figure 7(c) where no irreversible increase in the magnetic force is observed, at variance with the previous results.

The increase in the magnetic moment of the samples is also evidenced by the results for the magnetization isotherms at room temperature; cf figure 8. No significant changes in the magnetic hysteresis loops of the $Co_{10}Cu_{90}$ ribbons are observed upon heating the samples to 770 K (see figure 8(a)). However, the magnetic moment of the samples (at 300 K and in magnetic fields to 8×10^5 A m^{-1}) increases significantly upon heating the samples in the temperature range from 800 to 950 K; cf figure 8(b). This result agrees well with the steep increase of the magnetic force observed in the magnetothermogravimetric measurements.

The magnetization isotherms of the samples heated to 900 K are almost non-hysteretic, which confirms their superparamagnetic behaviour. Thus, the fitting of the magnetic moment of the sample annealed at 870 K to a Langevin function yields an average magnetic moment of the Co clusters of 6000 μ_B (see the inset of figure 8(b)) [26]. This value of the magnetic

moment of the Co clusters is of the same order of magnitude as the one obtained from the GMR measurements. This result reinforces the assumption of the presence of superparamagnetic Co nanoparticles, originating from heating the samples.

Heat treatments at temperatures above 950 K do not produce further increases of the magnetic moment of the heated ribbons (in magnetic fields to 8×10^5 A m^{-1}). Also, the magnetization isotherms from these samples show magnetic hysteresis, which is the fingerprint of the presence of larger magnetic particles that remain in a blocked state at room temperature. Due to their increase in volume, the thermal energy ($25k_BT$) is not sufficient to overcome the anisotropy barrier (KV) of the Co clusters. Therefore, the samples annealed to temperatures above 950 K do not show superparamagnetic behaviour at 300 K. The coercivity of the annealed samples is displayed in figure 4.

As mentioned above (see figure 4), the GMR of the melt-spun ribbons hardly increases upon heating the samples to 850 K. The GMR of the samples heated to above 850 K decreases, in the former measurement conditions. This decrease in the GMR of the heated samples is accompanied by the increase in the coercivity measured from the room temperature magnetization isotherms. This comparison would suggest that the highest values of the GMR are achieved in the early stages of the growth of the Co crystallites, when they behave like superparamagnetic particles. The further increase in the volume of the Co clusters as the heating temperature is increased gives rise to the increase of the anisotropy energy (K_uV) with respect to the thermal energy (k_BT). Thus, the magnetic clusters would experience blocking processes even at room temperature. The grain growth also gives rise to a reduction of the surface-to-volume ratio of the magnetic particles and consequently a decrease of the GMR.

4. Conclusions

The changes of the structure and magnetic properties of melt-spun $Co_{10}Cu_{90}$ ribbons upon heat treatments seem to be induced by the nucleation and growth of Co crystallites, a few nanometres in size. Heating the samples in the temperature range from 650 to 850 K induces irreversible changes of the resistivity of the samples as well as both a narrowing of the diffraction peaks in the x-ray diffraction pattern and a displacement of the diffraction maxima towards the positions for bulk Cu. In the former range of heating temperatures, the GMR of the heated samples also increases. The nucleation and growth of superparamagnetic Co nanoclusters as a result of the heat treatments could be the origin of the structural and magnetic changes.

Heat treatments above 850 K produce significant modifications of the magnetic moment of the samples (both measured by VSM in magnetic fields of 8×10^5 A m^{-1} and with a thermogravimetric analyser in an average magnetic field of 1.2×10^4 A m^{-1}). The intensity of the peaks corresponding to the (111) planes of the fcc Co also increases as the heating temperature increases. Also, on heating the $Co_{10}Cu_{90}$ ribbons above 850 K, the GMR starts to decrease, while the coercive field increases. These results could again be interpreted on the assumption of a further growth of Co crystallites. These nanocrystals would consequently be larger than the ones formed at lower temperatures. These larger Co clusters behave not as superparamagnetic particles but like blocked magnetic particles at room temperature, which gives rise to the decrease of the GMR.

Acknowledgment

This work was partly financed by the Spanish Comisión Interministerial de Ciencia y Tecnología (CICYT) within the project MAT98-0404.

References

[1] Berkowitz A E, Mitchell J R, Carey M J, Young A P, Zhang S, Spada F E, Parker F T, Hütten A and Thomas G 1992 *Phys. Rev. Lett.* **68** 3745
[2] Xiao J Q, Jiang J S and Chien C L 1992 *Phys. Rev. Lett.* **68** 3749
[3] Mitani S, Fujimori H and Ohnuma S 1998 *J. Magn. Magn. Mater.* **177–81** 919
[4] Pakhomov A B, Yan X and Xu Y 1995 *Appl. Phys. Lett.* **67** 3497
[5] Zhang S and Levy P M 1993 *J. Appl. Phys.* **73** 5315
[6] Rubinstein M 1994 *Phys. Rev.* B **50** 3830
[7] Wang J-Q and Xiao G 1994 *Phys. Rev.* B **49** 3982
[8] Wecker J, Von Helmolt R, Schultz L and Samwer K 1993 *Appl. Phys. Lett.* **62** 1985
[9] Madurga V, Ortega R J, Korenivski V, Medelius H and Rao K V 1995 *J. Magn. Magn. Mater.* **140–4** 465
[10] Ueda Y and Ito M 1994 *J. Appl. Phys.* **33** L1403
[11] Yavary A R, Desre P J and Benameur T 1992 *Phys. Rev. Lett.* **68** 223
[12] Madurga V, Ortega R J, Vergara J and Rao K V 1997 *Materials for Smart Systems (Mater. Res. Soc. Symp. Proc. vol 459)* ed E P George, R Gotthardt, K Otsuka, S Trolier-McKinstry and M Wun-Fogle (Pittsburgh, PA: Materials Research Society) p 483
[13] Hansen M and Anderko K 1985 *Constitution of Binary Alloys* (New York: Genium) p 469
[14] Childress J R and Chien C L 1991 *Phys. Rev.* B **43** 8089
[15] Childress J R and Chien C L 1991 *J. Appl. Phys.* **70** 5885
[16] Madurga V, Ortega R J, Vergara J, Elvira R, Korenivski V and Rao K V 1996 *Nanostruct. Mater.* **7** 185
[17] Miranda M G M, Bracho G J, Antunes A B, Baibich M N, Ferrari E F, da Silva F C S and Knobel M 1998 *Non-Crystalline and Nanoscale Materials* (Singapore: World Scientific) p 519
[18] Panissod P, Malinowska M, Jedryka E, Wojcik M, Nadolsky S, Knobel M and Schmidt J E 2000 *Phys. Rev.* B **63** 014408
[19] Madurga V, Ascasibar E, González J M, Morala M, García-Escorial A, Peces J A and Nielsen O V 1983 *Anal. Fís.* **79** 82
[20] Young R A 1996 *The Rietveld Method* ed R A Young (Oxford: Oxford University Press) p 9
[21] Cullity B D 1978 *Elements of X-Ray Diffraction* (Reading, MA: Addison-Wesley) p 102
[22] Cullity B D 1972 *Introduction to Magnetic Materials* (Reading, MA: Addison-Wesley) p 414
[23] Bean C P and Livingston J D 1959 *J. Appl. Phys.* **30** 120S
[24] Pfeiffer H and Schüppel W 1990 *Phys. Status Solidi* a **119** 259
[25] Vergara J, Ortega R J, Madurga V and Rao K V 1997 *J. Appl. Phys.* **81** 4596
[26] Madurga V, Ortega R J, Vergara J, Elvira R, Korenivski V and Rao K V 1995 *Magnetic Ultrathin Films, Multilayers and Surfaces (Mater. Res. Soc. Symp. Proc. vol 384)* ed E E Marinero, B Heinrich, W F Egelhoff Jr, A Fert, H Fujimori, G Guntherodt and R L White (Pittsburgh, PA: Materials Research Society) p 541